Level Set Trees with Enhanced Marginal Density Visualization

Kyösti Karttunen[1], Lasse Holmström[2] and Jussi Klemelä[2]
[1] *CEMIS-Oulu, Kajaani University Consortium, University of Oulu, Kajaani, Finland*
[2] *Department of Mathematical Sciences, University of Oulu, Oulu, Finland*
{*kyosti.karttunen, lasse.holmstrom, jussi.klemela*}*@oulu.fi*

Keywords: Explorative Data Analysis, Flow Cytometry, Kernel Density Estimation, Level Set Tree, Marginal Density, Mode Detection

Abstract: We study level set tree methods to analyze and visualize multivariate data. The probability density function of the underlying distribution is estimated using a kernel density estimator, and the density estimate is visualized using level set trees. These trees can be used to analyze the mode structure of a function. We show how level set trees can be used to enhance more traditional density function visualization tools, like marginal densities and slices of the density. The method is applied to flow cytometry data.

1 INTRODUCTION

Human conception of the surrounding world is effectively restricted to three dimensions. In the presentation of data we generally use only one or two dimensional (2D) structures for visualization, despite the existing but usually unusable 3D and 4D virtual reality environments.

Numerous methods have been developed to visualize multidimensional data, e.g. graphical matrices (Bertin, 1981), parallel coordinate plots (Inselberg, 1985), Andrew's curves, faces, the self-organizing map (SOM) (Kohonen, 1982; Vesanto, 1999), and scatter plots combined with projection pursuit and multidimensional scaling. The first decade of the personal computer age brought many of these methods into wider use. For an overview of these methods, see Klemelä (2009b, Chap. 1).

In this article we develop and apply a visualization method that is based on level set trees, introduced in (Klemelä, 2004).

This visualization method can be applied to data that are sampled from a continuous distribution. First, the probability density function of the observations is estimated, and then the level set tree based tools are applied to the density estimate. Density estimation based visualizations are an indirect way to visualize data, but they have at least two advantages: they are directly linked to making statistical inference about the underlying distribution, and they avoid the "curse of black ink", over-plotting resulting from displaying of large numbers of graphical elements.

Indeed, methods which represent every single observation with a graphical object, like scatter plots and parallel coordinate plots (PCP), cannot visualize a large number of observations without filling the paper or the computer screen. This can be avoided by using smoothing to estimate the underlying density. For example, in Fig. 2a a histogram density estimate is used instead of a scatter plot. For parallel coordinate plots, smoothing methods have been developed (Miller and Wegman, 1991) and density based plots are reviewed by Moustafa (2011). Alternatively, random subsetting can be used to avoid the "curse of black ink".

The density function of d-dimensional data is a d-dimensional function $f : \mathbb{R}^d \to \mathbb{R}$. Typically, multivariate density estimates are visualized using one- and two-dimensional marginal densities and slices (e.g. Scott, 1992). However, such visualization can be difficult. Marginal densities suffer from the problem that some features, for example modes, are sometimes masked in all one- and two-dimensional marginal densities. Slices suffer from the problem that we need a large number of them to visualize the complete multivariate density, and it is difficult to infer the features of the multivariate density from a large collection of one- and two dimensional slices.

Instead of marginal densities and slices we propose to use a level set tree (LST) based methodology. With the level set tree methods we can transform the multivariate density to a univariate density so that certain features remain invariant.

We are particularly interested in the modes of the density. Therefore we utilize a *voluplot*, which is a plot of a univariate density function that has the same mode structure as the original multivariate density function. By a mode structure we mean the number, the size, and the hierarchical tree structure of the modes. Finding modes of a density function can be applied for example in model based cluster analysis (e.g. Hartigan, 1975).

We use also *baryplots*, which visualize the level set tree by showing the locations of the modes and the centers of mass of all separated components of level sets. Additionally, we combine baryplots with the plots of estimates of marginal densities, and call these plots *enhanced marginal density plots*. Marginal densities are of course a well-known and widely used method and we can profit from combining it with a method which also shows the multivariate tree structure of the underlying density.

The LST-based methods are applied to flow cytometry data. Flow cytometry is an optical measurement technique that is used to measure biophysical and chemical characteristics of cellular particles (Melamed et al., 1994). We study the number of modes, their sizes and hierarchical structure from data, this time, originating from paper industry.

In Section 2, the concepts related to level set trees are reviewed. Section 3 illustrates the method with one- and a two-dimensional examples, and Section 4 presents the application to the flow cytometry data, and finally, Section 5 contains a discussion.

2 LEVEL SET TREES OF DENSITY ESTIMATES

We will first give the definition of a level set tree. Then we describe baryplots and voluplots, as well as point out how to combine marginal densities with the baryplots to obtain enhanced marginal plots. For a more precise and thorough description of these concepts, see (Klemelä, 2004; Klemelä, 2009b).

Level set trees, baryplots, and voluplots are calculated from kernel density estimates. A kernel density estimator is based on data $X_1,\dots,X_n \in \mathbb{R}^d$, assumed to be independent and identically distributed and originating from a common density function $f:\mathbb{R}^d \to \mathbb{R}$. The kernel density estimator of f is defined as

$$\hat{f}(x) = \frac{1}{n}\sum_{i=1}^{n} K_h(x - X_i)\,, \qquad (1)$$

where $K:\mathbb{R}^d \to \mathbb{R}$ is the kernel function, $K_h(x) = K(x/h)/h^d$ is the scaled kernel, and $h > 0$ is the smoothing parameter. We choose the kernel function K to be the standard normal density function. For more on kernel density estimation, see (Scott, 1992).

2.1 Level Set Tree

The *level set* $\Lambda(f,\lambda)$ of a function $f:\mathbb{R}^d \to \mathbb{R}$ at level $\lambda \in \mathbb{R}$ is defined as the set of those points where the function is greater than or equal to the value λ:

$$\Lambda(f,\lambda) = \{x \in \mathbb{R}^d : f(x) \geq \lambda\}\,. \qquad (2)$$

To construct a level set tree, we first choose a finite number of levels $\lambda_1 < \cdots < \lambda_L$. We assume that each level set $\Lambda(f,\lambda_l)$, $l = 1,\dots,L$, is either a connected set, or that it can be decomposed into a finite number of connected disjoint subsets,

$$\Lambda(f,\lambda_l) = \bigcup_{k=1}^{K_l} A_{lk}\,, \qquad l = 1,\dots,L\,, \qquad (3)$$

where $A_{lk} \cap A_{lm} = \varnothing$. The sets A_{lk} cannot be further decomposed into a union of disconnected components.

The root of a level set tree is the level set with the lowest level λ_1. If this level set has many disconnected components, then the level set tree has many roots. Given a node of a level set tree at level λ_l, the child nodes of this node are among the disconnected parts of the level set at one step higher level λ_{l+1}. The parent-child relation holds when the set associated with a child node is a subset of the set associated with the parent node.

The *level set tree* is a tree whose nodes are associated with levels λ_l and with the sets A_{lk}. The level set tree describes the local maxima (modes) of a density function, because the leaf nodes correspond to the local maxima.

2.2 Baryplots, Voluplots, and Enhanced Marginal Plots

The barycenter of set $A \subset \mathbb{R}^d$ is defined as

$$\text{barycenter}(A) = \frac{1}{\text{volume}(A)} \int_A x\,dx\,. \qquad (4)$$

Thus, a barycenter is a d-dimensional vector that defines the center of mass of a set. A *baryplot* is a plot of a level set tree that consists of d windows when the function is defined in the d-dimensional Euclidean space. Each window shows the positions of one coordinate of the barycenters for different levels:

1. the horizontal position of a node in the ith window is equal to the ith coordinate of the barycenter of the set associated with the node, where $i = 1,\dots,d$,
2. the vertical position of a node is equal to the level of the set associated with the node,

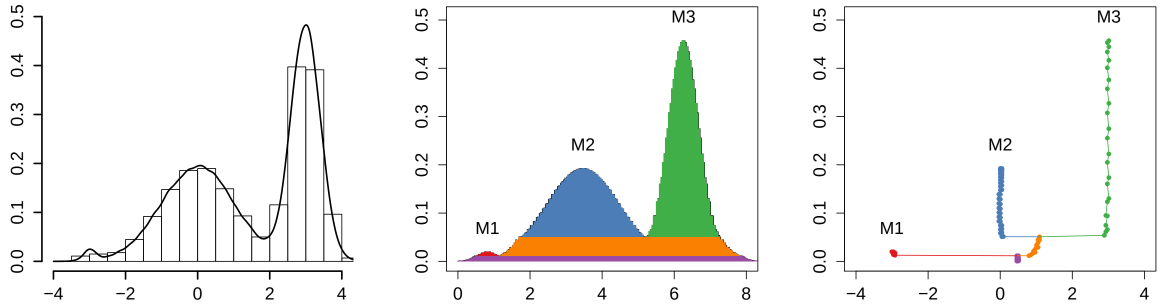

(a) Density estimates (b) Voluplot (c) Baryplot

Figure 1: Panel (a) shows a kernel estimate and a histogram estimate of a 1D density with three modes. Panel (b) shows a voluplot, and panel (c) shows a baryplot.

3. the parent–child relations are expressed by the line joining a child with the parent.

A baryplot visualizes the “skeleton” of the function, by displaying the 1D curves that go through the barycenters of all separated components of the level sets. An example of a baryplot is in Fig. 1c.

A *voluplot* is a second type of a plot of a level set tree. A voluplot gives information about the volumes of the disconnected parts of the level sets. The level set tree can be drawn in such a way that each node is associated with a horizontal line whose length is proportional to the volume of the set associated with the node. We construct a one dimensional function whose disconnected components of level sets are identical with those lines, and a voluplot is a plot of this one dimensional function. The envelope function shown in a voluplot is mode isomorphic with the original multivariate function in the sense that it has the same number of modes. The modes have the same size, and the hierarchical tree structure of the modes is preserved.

Finally, we will consider marginal densities and slices of a multivariate function. A one-dimensional marginal density $g : \mathbb{R} \to \mathbb{R}$ of a multivariate density function $f : \mathbb{R}^d \to \mathbb{R}$ is obtained by integrating out $d-1$ variables of f. For example,

$$g(x_1) = \int_{-\infty}^{\infty} \cdots \int_{-\infty}^{\infty} f(x_1, x_2, x_3, \ldots, x_d)\, dx_2 \cdots dx_d\,. \tag{5}$$

A one-dimensional slice $h : \mathbb{R} \to \mathbb{R}$ of a multivariate function $f : \mathbb{R}^d \to \mathbb{R}$ is obtained by fixing $d-1$ variables to a constant value, allowing only one free variable. For example,

$$h(x_1) = f(x_1, x_{20}, \ldots, x_{d0}), \tag{6}$$

where $x_{20}, \ldots, x_{d0} \in \mathbb{R}^{d-1}$ are fixed. Two-dimensional marginal densities and slices are defined analogously.

Multivariate density estimates are typically visualized by calculating marginal densities and slices of the estimates. We show below how to combine baryplots of density estimates with estimated marginal densities.

3 EXAMPLES OF LEVEL SET TREE PLOTS

3.1 A One Dimensional Example

LST tools were applied to visualization of one dimensional data in Fig. 1. We simulated $n = 40\,000$ observations from a mixture of three normal densities. Figure 1a shows a kernel density estimate together with a histogram density estimate. Figure 1b shows a voluplot, and Figure 1c shows a baryplot.

In the one dimensional case the voluplot is identical to the kernel density estimate, up to approximation errors and a difference in the location of the functions. The baryplot shows the level set tree together with the locations of the modes and the barycenters.

3.2 A Two Dimensional Example

Figure 2 shows an application of LST visualization to two dimensional data. We simulated $n = 10^5$ observations from a mixture of three normal densities.

Panel (a) shows a histogram with a hexagonal binning. With some effort, the three modes are discernible, but their presence is not obvious. Panel (b) shows a voluplot calculated from a kernel density estimate. The voluplot suggests three modes of clearly different heights as they branch at different levels. In the case of two modes the horizontal scale of the voluplot shows the distances of the modes in the original multidimensional Euclidean space. In panels (c)-(d) the baryplots are shown together with the marginals of the kernel density estimate. The labels M1, M2, and

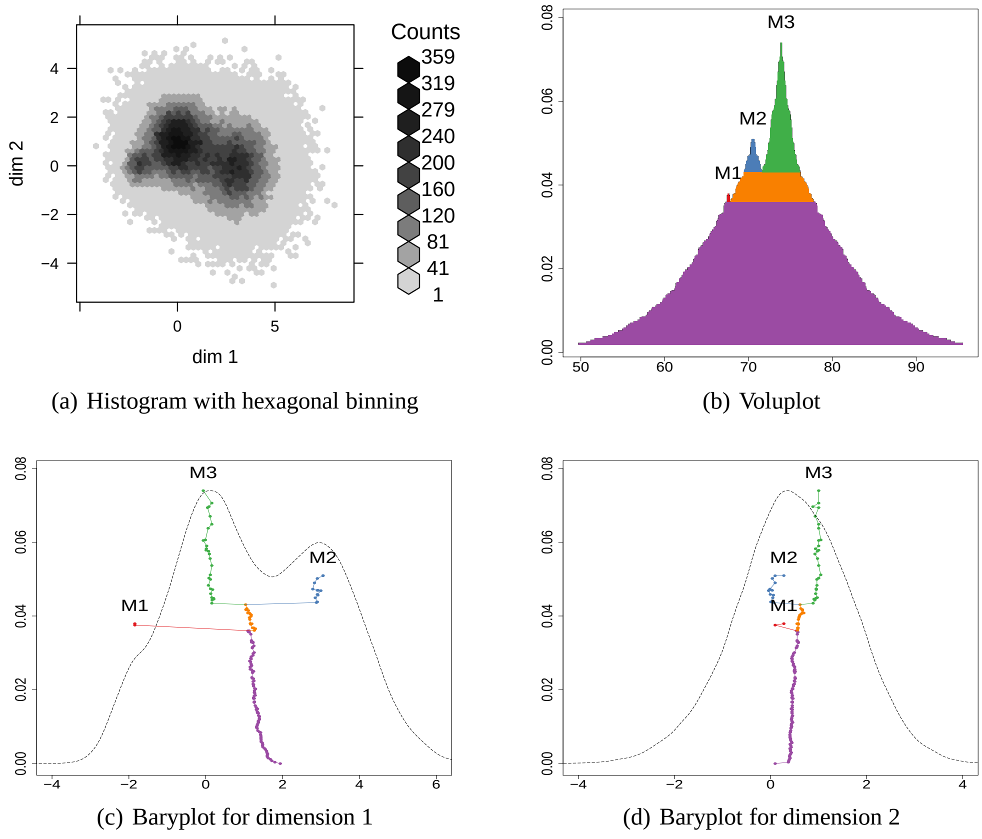

(a) Histogram with hexagonal binning (b) Voluplot

(c) Baryplot for dimension 1 (d) Baryplot for dimension 2

Figure 2: Panel (a) shows a histogram estimate with hexagonal binning of a three modal 2D density. Panel (b) shows a voluplot calculated form a kernel estimate, and panels (c) and (d) show the corresponding baryplots together with the estimated marginal densities.

M3 mark the modes. Note that the marginal density in panel (d) is unimodal, but the lines of the baryplot separate the three modes.

4 FLOW CYTOMETRY DATA - LST IN FOUR DIMENSIONS

4.1 Flow Cytometry

We analyzed laboratory data measured by a flow cytometer. Flow cytometry (FCM) is an optical measurement technique used typically to measure biophysical and chemical characteristics of thousands of cellular particles per second. The number of measured features per particle may vary from 2 to 16, and can be even higher in the state-of-the-art instruments. The general objective in FCM is to sort and classify particles (e.g. cells) into groups or clusters that can be used in the diagnosis of disorders, such as cancer, or HIV detection.

In addition to biomedical fields, FCM techniques are steadily expanding into other areas, too. For example, detection of some specific properties of wood pulp samples by using FCM techniques has been utilized by industrial research groups (Vähäsalo and Holmbom, 2005).

Despite the key role flow cytometers play in biomedical organizations, FCM data are typically analyzed using only two-dimensional dot or contour plots. While other approaches, such as parallel coordinate plots, can be used, the large number of particles involved restricts the usefulness of many methods. Still, careful and multifaceted inspection of FCM data is essential to maximize the information derived from the measurements.

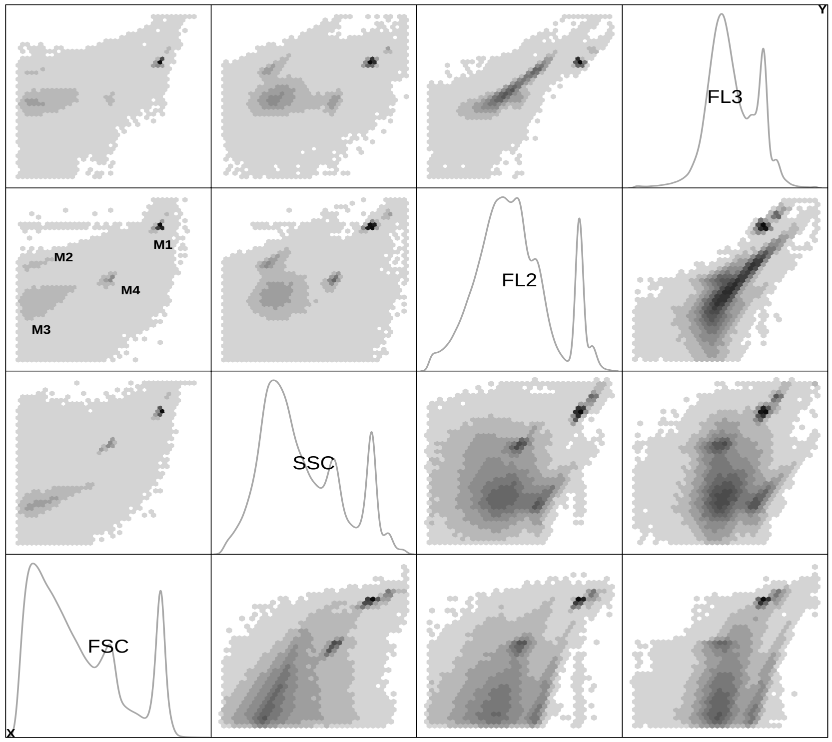

Figure 3: Scatterplot matrix and marginal densities of four dimensional FCM data are shown. Upper left pairs show linear density (gray) scale. In lower right pairs the density scale is square root, strongly emphasizing lower densities. Note that the data fill each graph since empty regions were left out. The M-annotations of the modes in one panel refer to Fig. 4.

4.2 Exploration of FCM data

Our FCM data originate from pulp and paper industry. Skipping the details of the arrangement and the practical relevance in the application, the measured pulp sample consisted of a mixture of irregular and round particles of different composition, such as fines (cut or crushed fibers) and pitch particles (resin). Furthermore, calibration particles of known diameter were added to the sample. The mean diameters of the two added monodisperse populations were $3\,\mu$m and $1\,\mu$m.

In our data analysis we consider four flow cytometry variables, also referred to as "parameters" or "channels", and named here FSC, SSC, FL2 and FL3. Physical significance of the variables are *forward scatter*, *side scatter* and two *fluorescence channels*, respectively.

4.2.1 Scatter Plot Matrix

A subsample of 161 264 observations of the measured FCM data set is shown in Fig. 3 as a scatter plot matrix, where the scatter plots have hexagonal bins. The observations with one component equal to zero were removed from the data, which resulted in the removal of 13% of the observations. Each variable was scaled to have range $[0,1]$. The marginal kernel estimates of the four variables are shown in the diagonal panels.

Several modes can be detected from these pairwise plots that suggest both wide and narrow structures in the data. However, these biplots represent only two dimensional marginal densities and may not be sufficient to capture all complexities in the data.

4.2.2 LST Method

Based on the particle type and physics in the measurement system, the particles were anticipated to create the following modal features in the measured data:

- calibration spheres: a narrow and dense mode in all coordinates,
- fines: a wide mode with tails,
- pitch: a clearly wider mode than spheres, but narrower than fines.

The kernel estimate, based on the FCM data, was evaluated on a grid of 24^4 points. The estimate has smoothing parameter $h = 0.05$ and the standard Gaussian density as the kernel function.

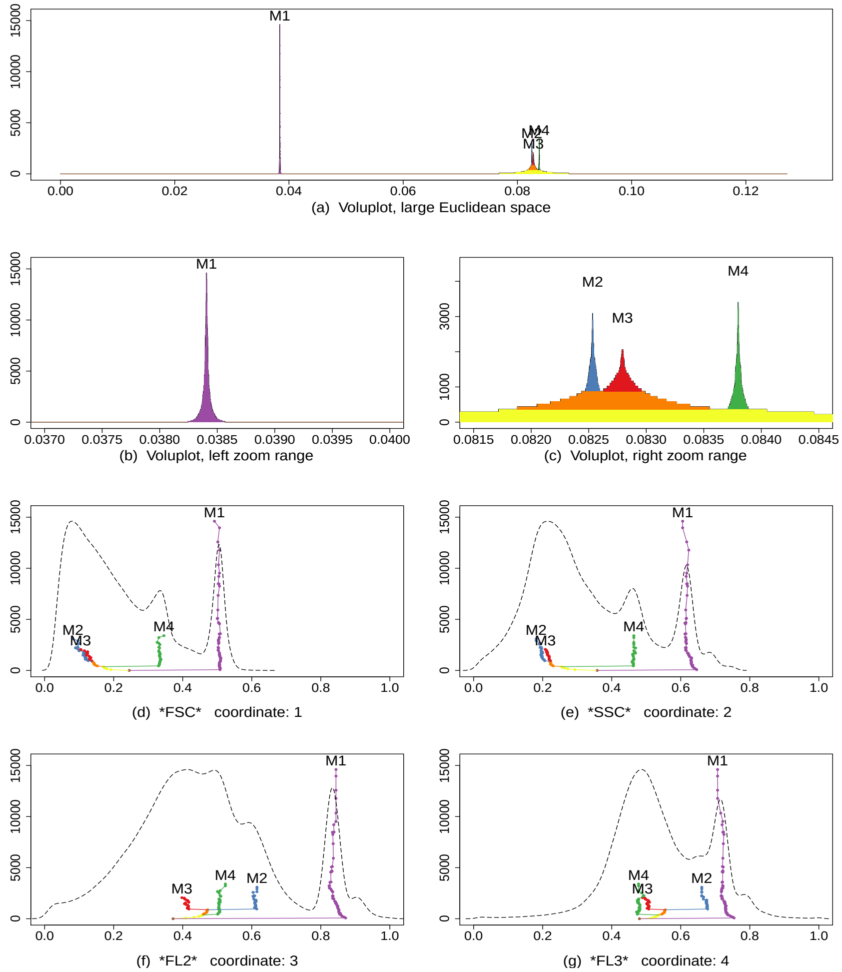

Figure 4: Four dimensional FCM data is visualized by LST voluplots and baryplots. Panel (a) shows the complete voluplot, and panels (b) and (c) zoom into details. Panels (d)-(g) show the four baryplots, one for each coordinate, together with the estimated marginal densities.

The result of subsequent LST data analysis is presented in Fig. 4 where one voluplot panel (a) and four baryplots, one for each dimension, are shown in panels (d)-(g). Figure 4a shows that most of the data are concentrated in the modes leaving much of the space empty – a reflection of the curse of dimensionality already visible in our relatively low-dimensional data set. In order to get a better idea of the modal structure, panels (b) and (c) zoom into to the relevant regions revealing various types of modes: wide (M3), narrow (M1, M4), low (M2, M3, M4), high (M1), all describing salient features of the four dimensional FCM data. These 4D modes are marked in one 2D marginal biplot in Fig. 3. To a varying degree, these modes are visible also in other biplots but the voluplot representation is much clearer.

A more detailed view of the modes and their positions is provided by the four baryplots in Figs. 4d–g. As in the voluplot, the highest level set M1 is easily identified. We may conclude that this nearly symmetric and narrow mode actually corresponds to the monodisperse 3 µm calibration particle population. Symmetry and relative narrowness indicate that the optomechanical measurement settings in the FCM unit functioned well. Likewise, the narrow, smaller mode M4 can be identified as the 1 µm calibration particle population.

The wide mode M3 (see Fig. 4c) clearly represents fines, and the slightly narrower M2 is caused by pitch. The skewness of M2 and M3 can be observed both from the scatterplot matrix and from the baryplots, but the baryplots quantify the degree and direction of skewness better.

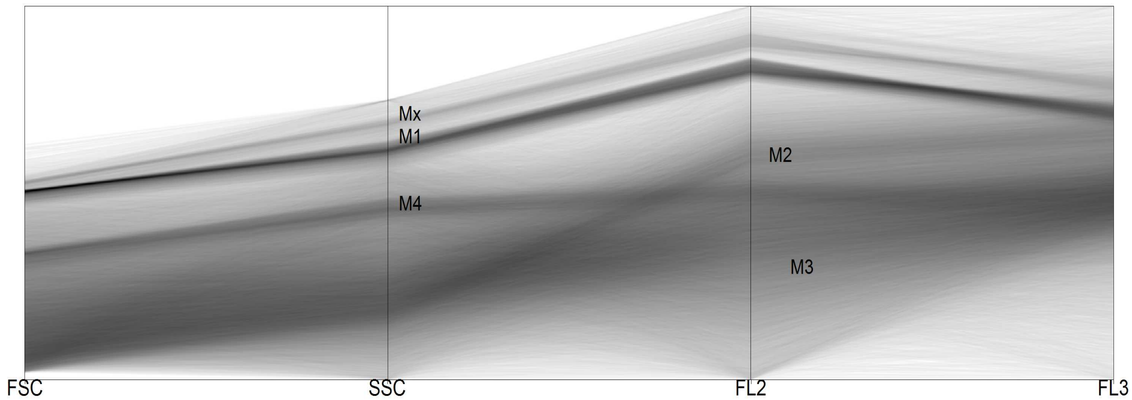

Figure 5: Density based parallel coordinate plot of the FCM data. The modes M1 to M4 are labeled to correspond to the ones in Fig. 4.

Finally, the marginal densities added to the baryplots in Figs. 4d–g complement the LST plots in useful way, facilitating the interpretation of baryplots.

4.2.3 Density Based Parallel Coordinate Plot

To compare the LST method with a more familiar multivariate visualization, we also created a density-based parallel coordinate plot of the FCM data (Fig. 5) as defined in Miller and Wegman (1991). The kernel density estimator was used with the standard Gaussian kernel and smoothing parameter $h = 0.0012$. We calculated 3000 univariate estimates, and evaluated each estimate on an equispaced grid of 1000 points. A subsample of 100 000 observations was used in the density plot.

In Fig. 5 the narrow modes M1, M2, and M4 can be distinguished and associated with the corresponding modes in Fig. 4. However, the wide mode M3, which is clearly apparent in the LST plots, is not easily observed in the PC plot. M3 appears as a smoothly varying background in the density-based PCP.

On the other hand, PCP suggests a mode Mx not reported in the LST analysis. Still, Mx can be visually observed in the enhanced baryplots as a shoulder of the marginal near M1, although not as a mode. This borderline case is due to the limited spatial resolution in the 4D density and level set calculations. At the same time it brings out issues in the LST visualization scheme that need to be addressed in future research, namely the need for efficient partitioning of the space as dimension increases.

Density based PCP nicely shows the connections of the modes in different dimensions. However, the structure of the modes, volume, shape, skewness, kurtosis, etc., cannot be observed as clearly as in the LST plots. In addition, the order of variables in the PCP may bias the inference to some extent as opposed to the equal treatment of the variables in the LST plots.

5 DISCUSSION

We have applied level set tree based methods to 4D flow cytometry data. In the four dimensional case it is possible to estimate density functions quite accurately, while the more traditional methods using marginal densities and slices are already difficult to use in this setting, and the difficulties would rapidly multiply if higher dimensional data were considered.

5.1 Observations – 2D or 4D

For our data, the modes can be detected both with the scatter plot matrix (2D) and with the LST plots (4D). However, the information provided by these methods is different. The scatter plot matrix is based on the histogram estimates of the two dimensional marginal densities, whereas the LST plots are based on the kernel estimates of the four dimensional density. Thus, the LST plots visualize the concentration of the probability mass in the 4D space instead of visualizing the concentration of the probability mass through projections to the 2D space, as is done in the scatter plot matrix. The existence and the location of the modes can be seen in the scatter plot matrix but the LST plots show estimates of the full mode structure of the underlying density. This means that we see estimates of the size of the modes and estimates on the spread of the probability mass associated with the modes. The scatter plots give indications of these properties, but since they show data projected to two dimensions (estimates of 2D marginal densities), we cannot infer the size of the modes and the spread of the probability mass in the 4D space. In FCM data analysis, the LST methods can simultaneously identify and quantify features of multidimensional particle clusters from large and dominating modes down to small and easily missed concentrations. This feature may prove to be highly valuable for example in medical FCM data exploration.

There are examples where the modes can be detected with the LST plots but not with the scatter plot matrices. This can happen when the modes are so close to each other that they mask each other in projections, see Klemelä (2004). On the other hand, scatter plot matrices may in some cases detect modes where the LST plots fail. This may happen when the number of variables (dimension of the observations) is so large that density estimation becomes intractable.

5.2 Clustering

Scatter plot matrices and parallel coordinates plots are not model based clustering methods. They need to be accompanied with a separate statistical technique to provide estimates and confidence statements about the mode structure. Mode detection with LST plots is an example of model based clustering. A voluplot gives an estimate of the so called excess mass of a mode. In our future work we plan to use this to associate statistical significance to the modes suggested by LST plots.

5.3 Finally

To conclude, the combination of voluplots and baryplots with marginal densities offers promising enhancements to more traditional visualizations and deepens the insight into the otherwise hidden multidimensional structures in data.

ACKNOWLEDGEMENTS

In addition to the R-code written by the authors, several R-packages were utilized (R Core Team, 2012; Sarkar, 2008; Klemelä, 2009a; Carr, 2011; Lemon, 2006).

This work has been partially supported by the Academy of Finland research project 250862 and by the Finnish Funding Agency for Technology and Innovation (Tekes) research project 40292/12.

REFERENCES

Bertin, J. (1981). *Graphics and Graphic Information-Processing*. De Gruyter, Berlin.

Carr, D. (2011). hexbin: Hexagonal binning routines. R package, ported by Lewin-Koh, N. and Maechler M.

Inselberg, A. (1985). The plane with parallel coordinates. *The Visual Computer*, 1(2):69–91.

Klemelä, J. (2004). Visualization of multivariate density estimates with level set trees. *Journal of Computational and Graphical Statistics*, 13(3):599–620.

Klemelä, J. (2009a). denpro: Visualization of multivariate functions, sets, and data. R package.

Klemelä, J. (2009b). *Smoothing of Multivariate Data– Density Estimation and Visualization*. Wiley, New York.

Kohonen, T. (1982). Self-organized formation of topologically correct feature maps. *Biological Cybernetics*, 43(1):59–69.

Lemon, J. (2006). Plotrix: R package. *R-News*, 6(4):8–12.

Melamed, M. R., Lindmo, T., and Mendelsohn, M. L. (1994). *Flow Cytometry and Sorting*. Wiley-Liss, New York.

Miller, J. J. and Wegman, E. J. (1991). Construction of line densities for parallel coordinate plots. In Buja, A. and O., T., editors, *Computing and Graphics in Statistics*, pages 107–123. Springer, New York.

R Core Team (2012). R: A language and environment for statistical computing.

Sarkar, D. (2008). *Lattice: Multivariate Data Visualization with R*. Springer, New York.

Scott, D. W. (1992). *Multivariate Density Estimation: Theory, Practice, and Visualization*. Wiley, New York.

Vähäsalo, L. and Holmbom, B. (2005). Influence of latex properties on the formation of white pitch. *Tappi Journal*, 4(5):27–32.

Vesanto, J. (1999). Som-based data visualization methods. *Intelligent Data Analysis*, 3(2):111–126.